SIX DEGREES OF FREEDOM MODEL FOR THE DYNAMICS OF HIGH ALTITUDE FLYING BODIES

Florin MINGIREANU[1], Lucian GEORGESCU[2], Gabriel MURARIU[2], Ionut MOCANU[2]

A typical six degrees of freedom (6 DOF) model is presented for the payload in order to allow a future implementation of controlled payload recovery through the usage of a steerable parafoil. Also an ascent rate calculation model is presented that takes into account a standard US 1976 atmosphere model as well as the thermodynamics of the lifting gas inside the weather balloon. We present the typical payload used as well as the APRS (Automatic Packet Radio System) communication package used for tracking and telemetry real-time as well as the photo and video equipment used for flight imaging. Altitude and trajectory are presented as functions of time and discussion is done regarding the best GPS (Global Positioning System) installation position in order to ensure GPS coverage data for most of the flight, including the burst. Various flight dynamics characteristics are described including the ascent and descent rates as well as a detailed description on how to achieve a desired ascent rate. Future aerosol detection mission is proposed in the framework of the next generation of satellites aimed at actively detecting aerosol pollution in the atmosphere. High altitude balloon platforms are proposed to provide calibration and validation of satellite data in various regions of interest worldwide. The flight data presented in this paper was obtained during nine high altitude flights performed in Romania, Australia and Finland.

Keywords: balloon, high, altitude, ascent.

1. Introduction

High altitude balloons are an inexpensive method of reaching altitudes from as low as 10 km to as high as over 50 km.[1] Nowadays, two main types of high altitude balloons are used:

- Rigid balloons
- Flexible latex balloons (e.g.: weather balloons)

Balloons are usually filled with helium or hydrogen which ensures the upward lift force generally decreasing with altitude.

One of the most used types of balloons is the flexible latex balloons which ensure expansion of the gas inside the balloon as the altitude increases. Upon reaching maximum expandable volume the latex balloon breaks apart and this breaking apart is described in the literature as the burst.

[1]Romanian Space Agency, Str. Mendeleev; Nr. 21-25, Bucharest, sector 1, 010362, Romania, E-mail: florin.mingireanu@rosa.ro
[2]University "Dunarea de Jos" of Galati, Romania, European Center of Excellence for the Environment (ECEE)

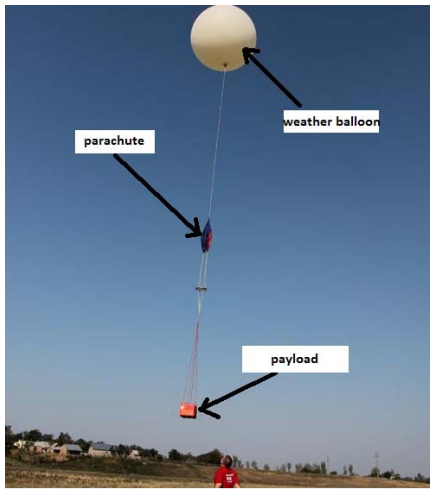

FIG. 1 High altitude balloon flight train

After the burst the payload returns to Earth by the means of a recovery parachute that decreases the descent velocity down to acceptable values. A typical descent velocity can be anywhere between 5m/s and 10 m/s depending on the type of equipment that the payload consists of.

The maximum altitude reached by a high altitude balloon was 53 km in 2012, reached by BU60-1. This balloon was of rigid type and the envelope was made of a 3.4 μm polyethylene film. The BU60-1 balloon was 34.37kg in empty weight, 74.5m in length, and 53.7m in diameter. The total weight including 0.8kg of parachute package and 4.6kg of observation instruments was 39.77kg.

2. Six degrees of freedom numerical model

We developed an in-house 6 DOF numerical simulation that allows modeling the attitude of the payload under the various forces that acts on it. This model is useful whenever one intends to integrate an inertial navigation unit (IMU) on the payload in order to recover attitude and position throughout the flight. The model is based on a general missile code that was developed also in-house by our research group.[2] The Earth's diurnal angular velocities are considered above basically as transport velocities for the transformation from one frame of reference to another.

Hence, with the above simplifications of non-rotating, flat Earth approximation, the translational equations of motion in tensor notation form become [4]:

$$mD^{B}v_{B}^{E} + m\Omega^{BE}v_{B}^{E} = F_{a,p} + mg \tag{1}$$

where $F_{a,p}$ is the vector sum of propulsive and aerodynamic forces along the given axis, m is mass, g is the gravitational acceleration, Ω^{BE} is the angular

velocity of body B relative to Earth's reference frame, v_B^E is the velocity of body B relative to Earth's reference frame.

We can write (1) in matrix coordinate form which makes them easier to be programmed on a computer:

$$\begin{bmatrix} \dot{u} \\ \dot{v} \\ \dot{w} \end{bmatrix}^B + \begin{bmatrix} 0 & -r & q \\ r & 0 & -p \\ -q & p & 0 \end{bmatrix}^B \begin{bmatrix} u \\ v \\ w \end{bmatrix}^B = \begin{bmatrix} F_x/m \\ F_y/m \\ F_z/m \end{bmatrix}^B + \begin{bmatrix} t_{11} & t_{12} & t_{13} \\ t_{21} & t_{22} & t_{23} \\ t_{31} & t_{32} & t_{33} \end{bmatrix}^{BL} \begin{bmatrix} 0 \\ 0 \\ mg \end{bmatrix}^L \quad (2)$$

where r, p, q represent angular velocities on pitch, roll and yaw axis, u, v, w velocity components in body frame, F_x, F_y, F_z resultant force components on the X, Y and Z axis. The matrix composed of terms t_{ij} rotates the gravitational acceleration vector from body reference frame to Earth's reference frame. Next we show the rotational dynamics equations which provide the relation between the aerodynamic and propulsive moments and angular accelerations of the rocket.

By applying Euler's law we have the following attitude dynamics equations in the body coordinates frame because the moments of inertia tensor has a simple and constant form in this reference system. We also have the attitude equations in quaternion formulation:

$$\begin{bmatrix} \dot{q}_0 \\ \dot{q}_1 \\ \dot{q}_2 \\ \dot{q}_3 \end{bmatrix} = \frac{1}{2} \begin{bmatrix} 0 & -p & -q & -r \\ p & 0 & r & -q \\ q & -r & 0 & p \\ r & q & -p & 0 \end{bmatrix} \begin{bmatrix} q_0 \\ q_1 \\ q_2 \\ q_3 \end{bmatrix} \quad (3)$$

where q_0, q_1, q_2, q_3 represent the quaternion components.

The quaternions are related to the Euler angles through the following well-known relations in the aerospace field [3], [4]:

$$\begin{aligned} q_0 &= \cos\left(\frac{\psi}{2}\right)\cos\left(\frac{\theta}{2}\right)\cos\left(\frac{\varphi}{2}\right) + \sin\left(\frac{\psi}{2}\right)\sin\left(\frac{\theta}{2}\right)\sin\left(\frac{\varphi}{2}\right) \\ q_1 &= \cos\left(\frac{\psi}{2}\right)\cos\left(\frac{\theta}{2}\right)\sin\left(\frac{\varphi}{2}\right) - \sin\left(\frac{\psi}{2}\right)\sin\left(\frac{\theta}{2}\right)\cos\left(\frac{\varphi}{2}\right) \\ q_2 &= \cos\left(\frac{\psi}{2}\right)\sin\left(\frac{\theta}{2}\right)\cos\left(\frac{\varphi}{2}\right) + \sin\left(\frac{\psi}{2}\right)\cos\left(\frac{\theta}{2}\right)\sin\left(\frac{\varphi}{2}\right) \\ q_3 &= \sin\left(\frac{\psi}{2}\right)\cos\left(\frac{\theta}{2}\right)\cos\left(\frac{\varphi}{2}\right) - \cos\left(\frac{\psi}{2}\right)\sin\left(\frac{\theta}{2}\right)\sin\left(\frac{\varphi}{2}\right) \end{aligned} \quad (4)$$

In order to determine attitude angles (yaw, pitch, roll) we use the inverse of relations (4) as follows:

$$\begin{aligned}\varphi &= \arctan\left[\frac{2(q_1q_2+q_3q_4)}{q_1^2-q_2^2-q_3^2+q_4^2}\right]\\ \theta &= -\arcsin[2(q_2q_4-q_1q_3)]\\ \psi &= \arctan\left[\frac{2(q_1q_4+q_2q_3)}{q_1^2+q_2^2-q_3^2-q_4^2}\right]\end{aligned} \tag{4'}$$

where θ represents the pitch angle, φ represents roll angle, ψ represents yaw angle. Based on the above quaternions one can write the full quaternion based transformation matrix from body to Earth reference frame:

$$[T]^{BL} = \begin{bmatrix} q_0^2+q_1^2-q_2^2-q_3^2 & 2(q_1q_2+q_0q_3) & 2(q_1q_3-q_0q_2) \\ 2(q_1q_2-q_0q_3) & q_0^2-q_1^2+q_2^2-q_3^2 & 2(q_2q_3+q_0q_1) \\ 2(q_1q_3+q_0q_2) & 2(q_2q_3-q_0q_1) & q_0^2-q_1^2-q_2^2+q_3^2 \end{bmatrix} \tag{5}$$

Next we can express the Euler equations in simple scalar form for easier programming on the computer through the following relations:

$$\begin{aligned}\dot{p} &= \frac{1}{I_1}[(I_2-I_3)qr+M_x]\\ \dot{q} &= \frac{1}{I_2}[(I_3-I_1)pr+M_y]\\ \dot{r} &= \frac{1}{I_3}[(I_1-I_2)pq+M_z]\end{aligned} \tag{6}$$

where M_x, M_y and M_z are the aerodynamic moments around body's x, y and z axis; I_1 is the axial moment of inertia, $I_2 = I_3$ are the lateral moments of inertia.

This 6 DOF model allows on one hand to simulate the dynamics of the payload under various forces and momenta. At the same time the same 6 DOF was implemented on an IMU in order to measure the dynamics of the payload during the flight and to keep track of the trajectory while comparing with the trajectory as measured by a GPS unit.

This IMU will allow in the future implementing an autonomous steerable parachute for the controlled recovery of high altitude balloon payloads. This will ensure the limitation of drift and will decrease the cost of recovery of such payloads.

3. Ascent dynamics model

An important parameter for high altitude flights is the ascent velocity. The ascent velocity is dependent on both the payload mass as well as the general

expected flight performances. One example is one the payload is required to have a certain altitude at a certain moment of time. Such an example is represented by our ECLIPSER-1 flight (November, 2012 - Australia) which needed to capture the eclipse at 25 km altitude and, hence, a precise timing had to be taken into account when computing the ascent rate and the time of launch.

We developed a 1-D model that predicts the ascent speed taking into account the atmosphere model, payload characteristics and some aerodynamics forces. For a payload hanged under a balloon we can write the equation of motion on vertical axis as follows:

$$F_{lift} - G - \rho v^2 S C_x \frac{1}{2} = 0 \tag{7}$$

where C_x axial aerodynamic coefficient, S is the cross section, v is the velocity and ρ is the local air density. In (7) we considered that weight **G**, lifting force $\mathbf{F_{lift}}$ and aerodynamic drag force **D** are the only forces that act on the balloon on the vertical axis. Important note is that in this particular situation, without incidence angle, the drag force **D** is identical to the axial force F_x from equation (2). We also ignored any dynamics on the horizontal axis due mainly the wind drifting. At equilibrium the ascent velocity is constant and, hence, the resultant of the above forces should be zero (right-hand side term is 0). That specific ascent velocity is the equilibrium ascent velocity which on average will be measured during that specific balloon flight mission. Also in (7) we assume that the gas inside the envelope expands isothermally and hence we can write the following equation for the gas expansion during an infinitesimal increase of altitude:

$$pV = const. \tag{8}$$

In equation (8), p is the local atmospheric pressure which is related to the altitude by the usual barometric relation:

$$p = p_0 e^{-\mu g h / kT} \tag{9}$$

where p is the pressure at a certain altitude, k is the Boltzmann constant, T is the temperature in Kelvin, g is the gravitational acceleration, h is the altitude, μ is the molar mass.

For the atmosphere profile we used the US 1976 standard atmosphere characteristics as given in [4] and included in Table 1.

Table 1

Standard US 1976 atmosphere- temperature profile

Altitude (meters)	Temperature (K)	Temperature lapse (K/m)
0	288.15	-0.0065
11000	216.65	0.0
20000	216.65	0.001
32000	228.65	0.0028
47000	270.65	0.0

By setting a certain amount of gas for a certain payload and balloon size we observe that we can obtain various values for the ascent velocities as given by equation (7).

As a conclusion of the above reasoning, the entire ascent of the balloon can be viewed as the isothermal expansion of the gas bubble represented by the balloon alongside with the dynamics generated by the expanding bubble and decreasing of air density with the increase of altitude.

4. High altitude balloon missions. Flight results and numerical modeling comparison.

A total of nine missions have been undertaken by our research group in order validate our solution for the payload, flight telemetry equipment as well as general launch procedures. First two flights were launched from Buzau city, Romania (October, 2011 and August, 2012) and represented the preparation for the third flight that took off from Queensland (near Zimba) Australia on November 2012. Additional of two flights were performed from Buzau in January and April, 2014 as well as four more missions in Finland with the specific purpose of measuring accurate six degrees of freedom payload dynamics through a dedicated IMU on which the above 6 DOF model was ran real-time.

Fig. 3, show the altitude as a function of time for STRATOSPHERIUM-1.

The horizontal axis represents time. At moment 200 we observe a dropout in telemetry data. This was produced by the positioning of the GPS module under a foam layer which in conjunction with the violent rotations of the payload after the burst (visible on the video recording) lead to a temporary loss of GPS signal.

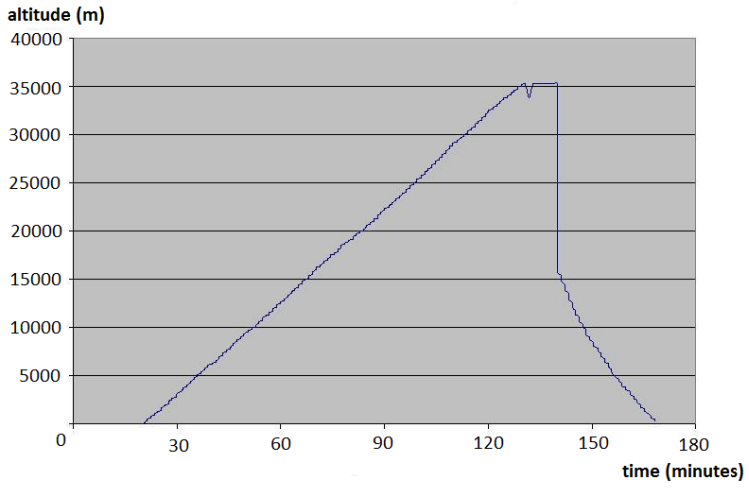

Fig. 3 Variation of altitude with time for STRATOSPHERIUM 1

The estimated ascent velocity based on our 1-D ascent velocity model was 6.2 m/s which is in good agreement with the measured ascent velocity was 5.83 m/s. For the calculation we used payload mass 3.7 kg, drag coefficient 0.2 and initial helium volume of 6.2 cubic meters.

Fig. 4 shows the trajectory of STRATOSPHERIUM-1 over the ground. In Fig. 4 we have the trajectory as received through APRS tracking system while in green we have the predicted trajectory using the 6 DOF model outlined in the previous chapter. We observe a very good agreement between the predicted trajectory and the real trajectory as determined during the flight. We can observe that the simulated trajectory (green track) is smoother than the real trajectory (red track) and this happens because average winds predictions are used rather than real wind data. It is important to note that the wind predictions are not 100% identical with the real winds from the day of flight and, hence, differences between the 6 DOF model and the real flight trajectory are to be expected. However, these differences are shown to be rather small in comparison to the range of the trajectory.

One step further was represented by the Finland flights. During these flights an IMU was installed onboard of the balloons and the above 6 DOF model was ran on the IMU throughout the flight.

Basically the 6 DOF model was ran real-time during the flight using the real wind data as measured during that specific flight. The trajectory as determined by the IMU (yellow trajectory) is basically the trajectory as determined by the 6 DOF model with real wind data- Fig. 5. This trajectory is then compared with the GPS trajectory (red trajectory) and a very accurate match is observed. Hence, our 6 DOF model as implemented for high altitude payloads is shown to be a high fidelity model well adapted to this type of flights usable on IMU applications.

Moreover the IMU was able to determine a series of attitude related parameters: pitch, yaw, roll angles as function of time. We can observe a very wide variation of all these parameters which is a sign of fast rolling, pitching and yawing dynamics. Despite this high dynamics the IMU was able to keep track of the trajectory proving that our quaternion based 6 DOF model is a sufficiently general model that allows modeling of flight dynamics with wide variation of flight parameters. The advantage of using the quaternion formulation is that we can avoid the typical trigonometrically singularities that would have prevented Euler based 6 DOF to work under this flight conditions.

The 6 DOF basically propagates an inertial solution based on gyroscope and accelerometer data provided by the IMU. Moreover, due to the inherent drift of the low cost gyroscope and accelerometers used in the IMU construction we drift-compensate the inertial data with GPS data every second.

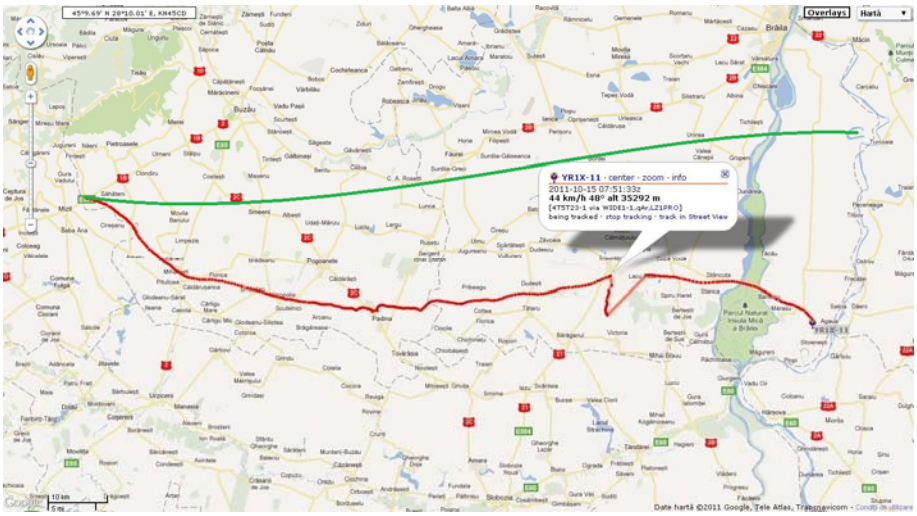

Fig. 4 Trajectory of STRATOSPHERIUM 1 as received by APRS network

Without this compensation the drift and bias of the gyroscope and accelerometers would provide false inertial solution and the trajectory as determined by IMU would slowly drift from the real trajectory. This drift and bias has nothing to do with the 6 DOF model; it is an instrumental error that is specific to the gyroscopes and accelerometers.

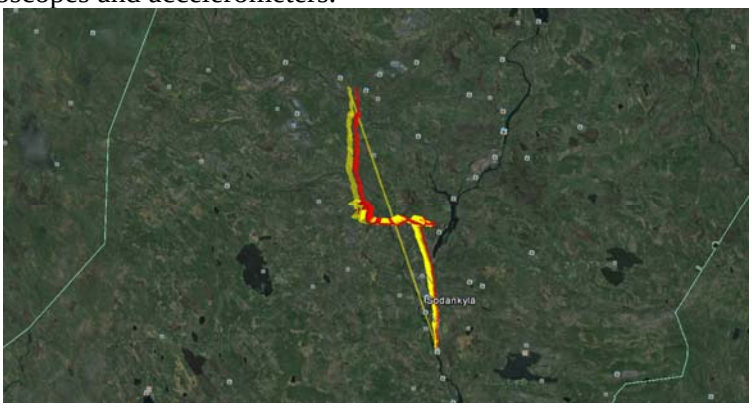

Fig. 4 Trajectory of Finland flight- IMU yellow; GPS red

In Fig. 5, 6 and 7 the horizontal axis represents the time in IMU time units. In order to convert the time from IMU time units to seconds one has to perform a multiplication by factor 0.288 of the IMU time units.

The reason for which we used IMU time units is because we did not want to perform additional operational on the onboard microcontroller. We used a time scale that was easier to maintain and use on the onboard microcontroller and then post-flight we would perform the conversion from the IMU time units to seconds.

As an example, one can observe in Fig. 5 that the roll dynamics settles down after ~25000 IMU time units which, through multiplication by 0.288 gives the result 7200 seconds which is the time from take-off to landing of that specific balloon mission.

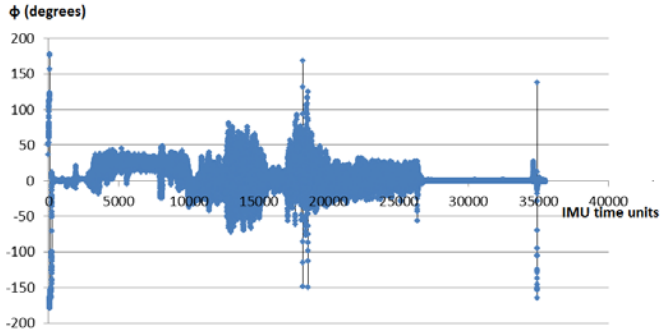

Fig. 5 Roll (φ) versus time

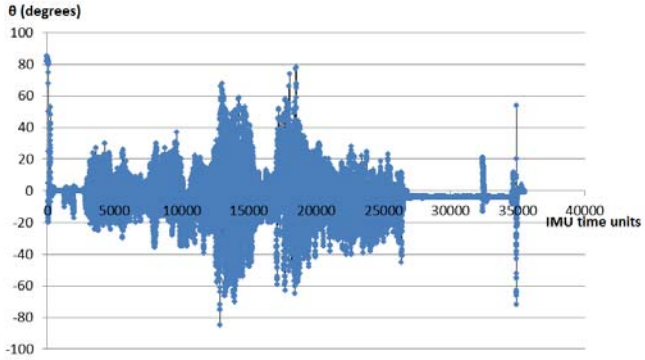

Fig. 6 Pitch (θ) versus time

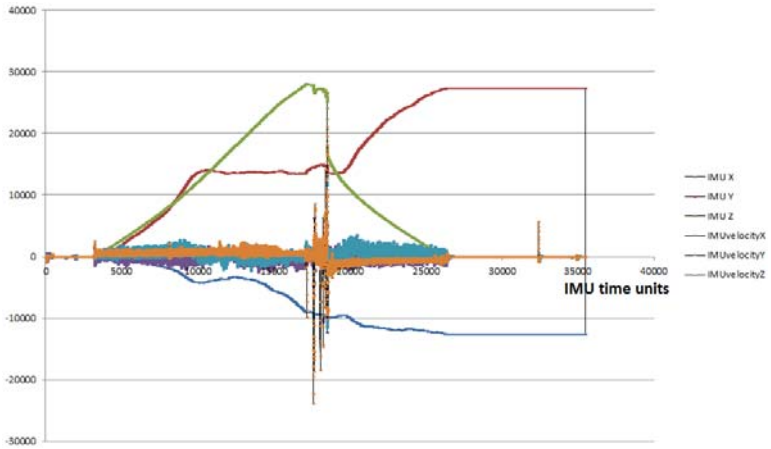

Fig. 7 Position and velocity components as determined by IMU

5. Conclusions

High altitude balloons are an inexpensive method of researching high altitudes and they are available on demand at mostly any point in the world. Satellites are more expensive and their data is not available on demand at anytime, anywhere. Through our work we developed an extensive 6 DOF model that is applicable to typical high altitude flights for both the ascent and the descent portions of the trajectory. We compared the 6 DOF trajectory estimations based on wind forecast with the actual trajectory recorded during a high altitude flight and found good correlation between the two. Next an IMU was shown to ran the 6 DOF model and provide accurate trajectory and attitude parameters. The 6 DOF ran real time on IMU with GPS drift compensation provides an excellent solution for both tracking and future recoverable steerable applications.

Next work will involve a complete model for the steerable parafoil as well as several test flights to validate the guidance algorithm.

Acknowledgements

Authors expressed gratitude to 3M and "Stiinta si Tehnica" magazine which supported this flight both financially and logistically.

Authors also express gratitude for the support offered by the Romanian Space Agency (ROSA) throughout the research effort.

At the same time authors are also grateful for the support and research guidance offered by University "Dunarea de Jos" of Galati, Romania, European Center of Excellence for the Environment (ECEE) through POSDRU 76822.

R E F E R E N C E S

[1] *A. Nayak, A. G. Sreejith, M. Safonova, Jayant Murthy*, High altitude ballooning program at the Indian Institute for Astrophysics, Current Science, Vol. 104, No. 6, 25 March 2013

[2] *M. Khalil, H. Abdalla* and O. Kamal,* "Trajectory Prediction for Typical Fin Stabilized Artillery Rocket" ", Proceedings of the 13th International Conference on Aerospace Sciences and Aviation Technology, ASAT-13," May 26-28, 2009

[3] *Pawat Chusilp, Weerawut Charubhun, and Navapan Nutkumhang.* „A Comparative Study on 6-DOF Trajectory Simulation of a Short Range Rocket using Aerodynamic Coefficients from Experiments and Missile DATCOM", The Second TSME International Conference on Mechanical Engineering, 19-21 October, 2011, Krabi

[4] *Peter Zipfel,* „Modelling and simulation of aerospace vehicle dynamics", AIAA, 2000, ISBN 1-56347-456-5